

PHOTORESIST RESIDUE DETECTION IN ADVANCED PACKAGING

Jonathan Cohen, Woo Han Young, Gurvinder Singh, Keith Best, Amy Shay, Mike Marshall
Rudolph Technologies, Inc.
4900 West 78th Street
Bloomington, Minnesota 55435
Ph: 952-820-0080; Fax: 952-820-0060
Email: Gurvinder.Singh@rudolphtech.com

Abstract

Semiconductor manufacturers are continuously driving efforts to put more computing power and speed into less volume. At the same time, consumers are demanding devices with more functionality that integrate a variety of interconnected circuit types. The result has been an increasing reliance on advanced packaging technologies that use fab-like processes to integrate multiple chips and to provide the increased I/O capability required. With continued focus on device miniaturization, the rapid detection of trace chemical residue during intermediate processing steps becomes increasingly difficult. In the lithography area, detection of polymer residue on wafer surfaces presents special opportunities. One area of opportunity for the detection of lithographic polymer residue takes advantage of the fact that these materials possess unique optical properties not found in metals or other inorganic materials used in semiconductor manufacturing. Rudolph Technologies has submitted patent applications for a novel defect illumination technique that offers key advantages over traditional white light inspection. This paper will present the results of using this inspection technique for the detection of photoresist residue on test wafers as well as on actual customer devices. Sample data included herein are representative of advanced packaging technology used today by a wide range of semiconductor manufacturers and OSAT facilities. While this novel inspection technique will not be a panacea for all trace residue detection problems, it offers a method complementary with bright field or dark field inspection when these two traditional inspection methods lack the sensitivity required.

Key words

Advanced packaging, inspection, photoresist, residue, FOWLP, Clearfind

I. Introduction

With the advent of 21st century digital devices, such as smartphones, tablets, internet-enabled data monitors, augmented reality interfaces, and autonomous vehicles, consumers demand increasingly sophisticated capabilities from smaller and smaller devices. From a manufacturing standpoint, this will require advanced packaging techniques that combine multiple individual devices, often built upon separate substrates, into a single, discrete package with increasingly complex I/O interfaces. At the same time, these devices will continue to shrink in accordance with Moore's Law [1], requiring ever tighter tolerances for defects within the process flow.

With continued focus on device miniaturization in the advanced packaging world, the detection and removal of

trace chemical residue during intermediate processing steps becomes increasingly difficult. In the area of lithography, manufacturers of ultra-large-scale integrated devices are demanding defect inspection solutions capable of detecting and classifying 1.0 μm and even sub-1.0 μm quantities of chemical residue.

Recently, Rudolph Technologies, Inc. has introduced a novel macro defect inspection platform that uses patented illumination technology for the detection of microscopic quantities of organic contaminants on semiconductor wafers. The new method takes advantage of the fact that many organic polymers used in modern lithography exhibit distinctive optical properties not present in metals, silicon, or other common inorganic materials used in semiconductor manufacturing. These properties tend to be unique to organic molecules displaying a high degree of conjugation, such as in polycyclic aromatic hydrocarbons and in linear or

branched-chain organic polymers with multiple, regularly interspersed pi-bonds [2].

Rudolph Technologies' novel inspection technique offers benefits not available through traditional white light inspection systems. Firstly, the illumination technique will present a high color contrast against a metallic or other inorganic surface. Secondly, defect emission tends to be anisotropic and therefore less sensitive to surface patterning that could potentially direct most ordinary bright field or dark field reflected light at angles away from the detection optics. As a result, the inspection is more sensitive to trace residue of interest while being less sensitive to interference from the surrounding features.

In this paper, the authors present data demonstrating the value of this patented inspection technology to detect commonly encountered lithography materials both as blanket films and as residue found on patterned wafers representative of advanced packaging technology used today. The data will show that this new technique offers a method complementary to white light based bright field or dark field inspection when these traditional inspection methods lack the sensitivity required.

II. Materials and Methods

All inspection data presented in this paper were collected using a Rudolph Technologies Firefly™ macro defect inspection system attached to a two-loadport XCluster™ wafer handler.

Simplified illustrations comparing the patented Clearfind™ technology to traditional white light inspection systems are shown in Fig. 1.

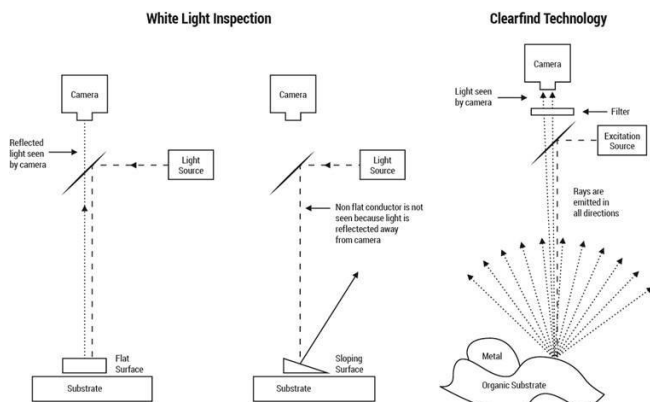


Fig. 1: Simplified illustrations of the differences between traditional white light inspection systems and Clearfind technology.

The light source for Clearfind technology is laser based

rather than relying on a broadband light bulb used in white light inspection systems. Thus, the light output is more stable in terms of both spectral range and output power. The laser output beam is collimated and expanded into a horizontal line at the sample. A wavelength filter is placed in the optic path after the inspection objective to remove any reflected laser light from reaching the imaging camera. In this paper, the authors present data collected at 4X and at 10X magnifications. At 4X, the laser line dimensions at the sample are approximately $7.1 \times 44 \text{ mm}^2$ and at 10X are approximately $2.8 \times 18 \text{ mm}^2$.

Autofocusing of the samples was accomplished using a patented, high speed, NIR-based laser triangulation system that maintains a constant distance between the imaging optics and the area being scanned [3].

Imaging of the sample was accomplished using a high resolution line scan camera. The nominal image magnification at 4X and at 10X is equal to $1.4 \mu\text{m}/\text{pixel}$ and $0.7 \mu\text{m}/\text{pixel}$, respectively.

The bright field inspection results using a white light source at 4X were obtained on the same Firefly inspection platform used for Clearfind inspection by methods described elsewhere [4].

Sample placement, magnification, illumination intensity, camera gain, image processing and defect detection configuration were accomplished using Rudolph Technologies' XSoft™ software. Defect image analysis was performed using Rudolph Technologies' Discover® Client software.

PW1000T and AZ4620 photoresist samples were prepared by Rudolph Technologies on 200-mm Si substrates using a JetStep® W stepper. Exposure was accomplished using the ghi Hg emission wavelengths and 0.1 NA. A progressive series of $\sim 1.0 \times 1.0 \text{ cm}^2$ dose-to-clear (DTC) windows were created on the wafers using varying dose energies from 100-340 mJ in 2 mJ steps. No reticle bias or focus offset was applied during exposure. Exposure was followed by a soft bake and development using a dilute TMAH solution.

The 300-mm patterned production wafer sample was prepared by a leading memory manufacturer producing devices for the 14 nm technology node.

III. Results

PW1000T Photoresist Sample

To test the ability of Clearfind technology to detect trace quantities of residue, flat film samples of PW1000T

photoresist were prepared using methods described in section II. The thickness of the photoresist films within the DTC windows was verified by multiple angle of incidence, focused beam ellipsometry using methods described elsewhere [5]. For each thickness of PW1000T deposited onto the DTC window the inspection tool measured the grayscale value (GSV) of the film when exposed to Clearfind illumination. The results are shown in Fig. 2.

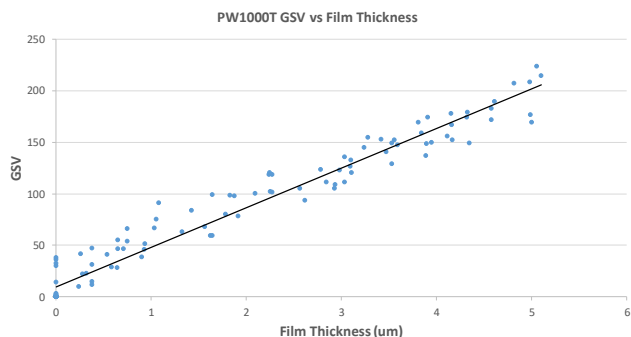


Fig.2: Scatter plot of PW1000T GSV intensity versus film thickness. R-squared linear least squares fit to the data is equal to 0.9589.

The data in Fig. 2 shows that there is a strong linear correlation between the GSV intensity and the thickness of the photoresist when exposed to Clearfind illumination. In the absence of photoresist, the GSV intensity of the underlying Si substrate using Clearfind is less than 20. However, the Clearfind GSV intensity of PW1000T is greater than 50 even at film thickness values approaching 1-2 μm . This demonstrates that even for minute quantities of photoresist Clearfind inspection is capable of distinguishing the presence or absence of residue down to the micron level.

AZ4620 Photoresist Sample

Like the PW1000T sample, a similar sample of AZ4620 resist was prepared using methods described in section II. Likewise, for each dose/thickness of AZ4620 deposited onto the test wafer the inspection tool measured the GSV intensity of the film when exposed to Clearfind illumination. For the AZ4620 sample the thickness of the film was verified by white light interferometry [6]. The results are shown in Fig. 3.

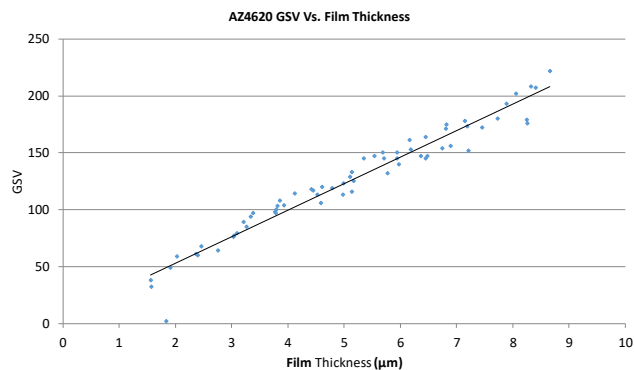


Fig. 3: Scatter plot of AZ4620 GSV intensity versus film thickness. R-squared linear least squares fit to the data is equal to 0.9593.

Like the PW1000T data shown in Fig. 2, the data in Fig. 3 shows that there is a strong linear correlation between the GSV intensity and the thickness of the AZ4620 photoresist when exposed to Clearfind illumination down to film thickness values approaching 2 μm . In the absence of photoresist, the GSV intensity of the underlying Si substrate using Clearfind is less than 20. However, the Clearfind GSV intensity of AZ4620 is greater than 50 even at film thickness values approaching 2 μm . Note, there is one gross outlier point near 1.75 μm in the Fig. 3 data that shows a GSV intensity value equal to zero. The AZ4620 films are thick and not very uniform over small areas of some DTC windows. The authors believe the thickness measurement at this site by the interferometer is erroneous. Nevertheless, the data in Figs. 2 and 3 demonstrate that even for minute quantities of photoresist Clearfind inspection is capable of distinguishing the presence or absence of residue down to the micron level.

The purpose of the PW1000T and AZ4620 GSV intensity versus thickness experiments was not to use Clearfind technology to measure film thickness. Rather, the purpose of these tests was to demonstrate that Clearfind technology can be used to detect the presence or absence of photoresist residue even when the residue is on the order of 1-2 μm . The changes in GSV intensity of the photoresist relative to the substrate background intensity are sufficiently large using Clearfind illumination that an automated detection system based on differences in GSV values by pixel can be established.

Product Data

The value of Clearfind technology is best demonstrated by its ability to detect trace lithographic chemical residue on actual product wafers generated in a semiconductor fab. To accomplish this, a 300-mm patterned Si wafer from a large memory manufacturer was inspected. The product wafer inspected consists of dies approximately 11.7 x 7.6 mm^2 that contain arrays of ~9000 metal pillars, each approximately 22

μm in diameter. The customer was very interested to learn if residual organic matter on the surfaces of the pillars could be detected. The customer also wanted to learn if Clearfind inspection is able to detect defects missed by the white light inspection method. Fig. 4 shows a Clearfind image of the device. Each die was inspected twice; once using a white light source operating in bright field and a second time using Clearfind technology. A dark field inspection was not practical in this case because the surfaces of the pillars were too reflective to be able to effectively image defects. The inspection magnification was set equal to 4X (1.7 μm/pixel) and review images were captured at 10X magnification (0.7 μm/pixel) to better highlight the defects. Circular inspection regions of interest were created to overlap with each pillar on each die. Any anomalies greater than 5 μm were classified as defects. The bright field and Clearfind inspections use identical algorithms for wafer placement and pattern alignment so that defects common to both inspections will overlap on subsequent defect maps.

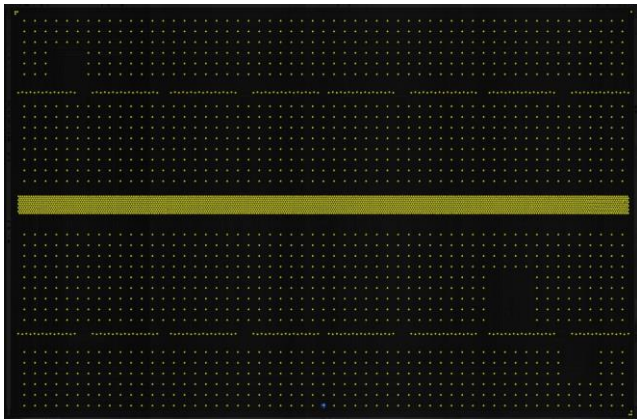


Fig. 4: Clearfind image of the device die for pillar inspection. Yellow dots represent pillar ROIs for inspection.

An overlay map of the bright field defects and the Clearfind defects is shown in Fig. 5. Bright field defects include random particles, broken pillars, incompletely patterned areas, scratches and other commonly encountered defects scattered throughout the wafer. Similarly, Clearfind inspection identifies defects distributed randomly across the wafer and are not observed to be clustered in any one particular area on the wafer or within a given device.

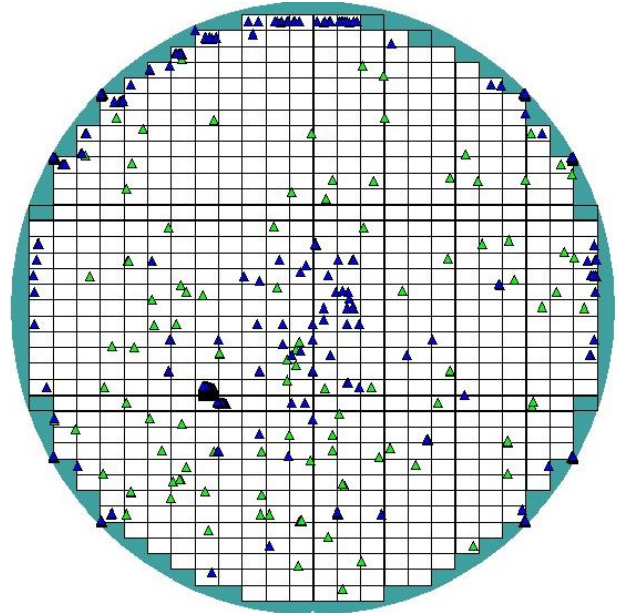


Fig. 5: Overlay map of defects found on the production devices described in Fig. 4. Blue triangles represent bright field defects. Green triangles represent Clearfind defects.

A bar chart showing the total defects found by bright field inspection versus the total defects found by Clearfind are shown in Fig.6. Also shown in Fig.6 are the number of defects found during Clearfind inspection that are common to both bright field and Clearfind inspection. The results of the 4X inspection show 2279 total defects found in bright field inspection and 289 total defects found in Clearfind inspection. Of the 289 Clearfind defects only 32 of them were also found by bright field inspection, the remaining 257 were unique to Clearfind inspection, representing 10.1% of the total defect count. As a result, a defect inspection protocol only using bright field would have missed many possibly killer defects that could have led to subsequent device failure or costly rework of the wafer.

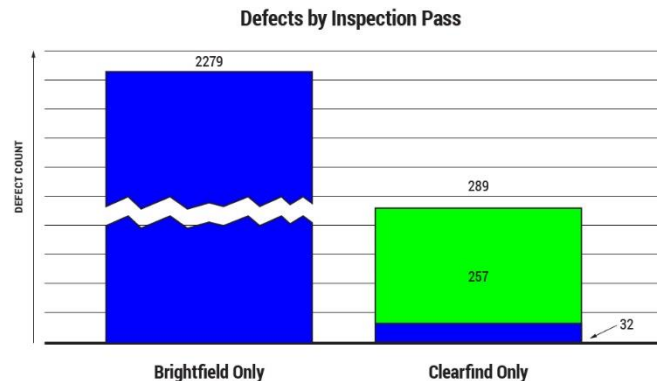


Fig. 6: Bar chart showing the number of defects found by bright field inspection, the number of defects found by Clearfind inspection, and the number of defects common to both inspections for the devices inspected in Fig. 4.

Review images of the defects found only in Clearfind inspection were generated at 10X magnification to compare against the identical bright field images of the same area on the devices. A sample of paired bright field and matching Clearfind images is shown in Fig.7. Defects found in these Clearfind images span sizes from approximately 7.2 μm to 13 μm . Each pair of images show that defects missed in the bright field inspection are very easy to detect and to visualize in the corresponding Clearfind images. The enhanced brightness and circular shape of the Clearfind defects shown in Fig. 7 strongly imply that these defects are associated with polymer residue. The enhanced brightness of the defects in the Clearfind images against a very black background is a unique and valuable feature of Clearfind inspection. Surfaces that are very rough, very reflective, or show a complex surface pattern will not interfere with the ability of Clearfind inspection to locate defects because only Clearfind photons are allowed to pass through the filter and reach the camera.

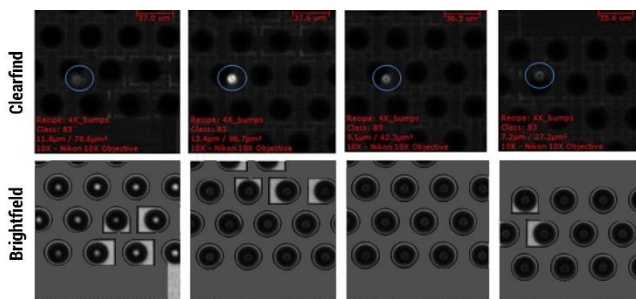


Fig.7: Example review images of Clearfind defects that were missed by bright field inspection. All images were captures at 10X magnification (0.7 μm /pixel).

IV. Conclusion

The data shown here prove the benefits of supplementing traditional white light inspection techniques with Clearfind inspection. Clearfind technology allows for the selective illumination of organic residue on surfaces without interfering signals from the background. The DTC data presented here show that detection of the presence of residual photoresist or other lithographic chemicals can be extended to the micron and possibly the submicron range. Data obtained on actual device wafers prove that defects that may be missed by a white light inspection pass can be easily detected and visualized in a Clearfind inspection pass. While Clearfind technology will not be a panacea for all trace residue detection problems it offers a method complementary to traditional white light inspection methods when those methods lack the desired sensitivity.

The data presented in this paper focuses primarily on the benefits of Clearfind technology to detect surface defects on pillars or other structures above the wafer surface. Future papers will focus on the ability of Clearfind technology to detect defects within vias or other high aspect ratio structures that lie beneath the nominal wafer surface.

Acknowledgments

The authors wish to acknowledge Corey Shay and Jack Mach of the Rudolph Technologies Lithography Systems Group for their assistance in preparation of the PW1000T and AZ4620 samples, Ben Meihack and Duncan Stelzer of the Rudolph Technologies Product Control Group for their assistance with Clearfind recipe setup and data review, and Jian Ding of the Rudolph Technologies Metrology Business Unit for helpful technical insights on the Clearfind optical system.

References

- [1] G. E. Moore, "Cramming more components onto Integrated Circuits", *Electronics*, vol. 38, Apr. 1965, 114–117.
- [2] D. C Harris, M. D. Bertolucci, *Symmetry and Spectroscopy*, Dover Publications, New York, 1978, pp. 307-418.
- [3] R. Bishop, T. Pinkney, "High Speed Autofocus System", U.S. Pat. App. Pub. 2014/0104409 Apr. 2014.
- [4] N. Devanciard, D. Allia, "Combining defect detection/metrology to accelerate micro-bump/pillar fabrication," *Chip Scale Review*, Jan/Feb, 2016, pp. 21-25.
- [5] Rudolph Technologies, Multiple-Angle Incidence Ellipsometry Measures Very Thick Films, <https://www.laboratorynetwork.com/doc/multiple-angle-incidence-ellipsometry-measure-0001#met>.
- [6] R. Roy, T. Kryman, R. Asgari, "Metrology and Inspection Solutions for TSV Processes Used to Connect 3D Stacked ICs", *Chip Scale Review*, Nov/Dec, 2012, pp. 37-40.